Physics Open 10 (2022) 100098

Contents lists available at ScienceDirect

Physics Open

journal homepage: www.elsevier.com/locate/physo

Quantum gravity at the fifth root of unity

Marcelo Amaral *, Raymond Aschheim, Klee Irwin

Quantum Gravity Research, Los Angeles, CA, USA

ARTICLE INFO

Keywords:
Quantum gravity
Spin foam
Unification physics
Topological order

ABSTRACT

We consider quantum transition amplitudes, partition functions and observables for 3D spin foam models within $SU(2)$ quantum group deformation symmetry, where the deformation parameter is postulated to be a complex fifth root of unity. By considering fermionic cycles through the foam, we couple this $SU(2)$ quantum group with the same deformation of $SU(3)$ so that we have quantum numbers linked with spacetime symmetry and charge gauge symmetry in the computation of observables. In this case, the amplitudes have a polytope interpretation. The generalization to higher-dimensional Lie groups $SU(N)$, G_2 and E_8 is suggested.

1. Introduction

Quantum gravity and unification physics programs, in the absence of more concrete experimental results, rely much on rigorous mathematical results to make progress. The well established quantum gravity programs of loop quantum gravity (LQG) [1] and string theory [2,3] are good examples of this new paradigm to find clues about the underlying physics at the Planck scale. For a review of the motivations and main results of LQG and spin foam models we recommend the book [1]. We also recommend a review of the main elements of the higher dimensional Lie algebra unification program [4–8], which is closely related to string theory. With these results as guides, this paper will construct a model where quantum numbers associated to quantum geometry or spacetime symmetry in usual $SU(2)$ spin foam models in 3D are coupled with eigenvalues of operators from higher dimensional Lie algebras, which can be associated to "charge" quantum numbers. This is done by defining 3D topological observables.

It is interesting to point out that LQG starts from general relativity and provides its quantization, which leads to the quantization of the geometry itself; lengths, areas and volumes, in operator form, have discrete spectra; they have minimum quanta. But it does not incorporate matter and the quantum fields — the charge space symmetries. On the other side, string theory starts from the quantum fields and implements the generalization from point particles to extended particles, like a one dimensional string or the higher dimensional branes. This also leads to discrete spectra, and a more complete description of unification physics. But this unification picture is more complicated because the strings are defined over a spacetime manifold, which leads to fundamental problems and the search for a more fundamental ($M-$)theory, where "one hopes to understand the existence of a spacetime manifold itself as the emergent property of a specific vacuum rather than an identifiable feature of the underlying theory" [3]. A partner approach of string theory, but less ambitious, is the Lie algebraic unification program, as in E_8 unification [9,10]. This makes use of the generalization of the simplest non-abelian gauge symmetry, $SU(2)$, to higher-dimensional ones, ending with a complete unification of the charge Lie group symmetries of the standard model in the largest exceptional Lie algebra E_8, making heavy use of the representation theory of these algebras. Our aim is to use this unification aspect of the representation theory of Lie algebras in connection to the spin foam approach of LQG. We can say that spin foam partition functions or transition amplitudes are about the interaction of representations of spacetime symmetry, and so, ultimately, E_8 can provide the network of interaction representations incorporating the usual charge symmetries — but here we focus on the first step in 3 dimensions where spacetime symmetry is just $SU(2)$ and internal charge symmetry is chosen to be $SU(3)$. We also provide a polytope interpretation for the representations of charge symmetry in the spin foam network[1].

Both the LQG and string/M-theory programs lead to the idea of building blocks for all the fields that constitute our classical and quantum worlds, from which the question arises of how to "glue" these fundamental blocks together in an elementary and first-principles way. There have been recent efforts to use the idea of entanglement in both approaches [11,12].

In the model we develop here, the building blocks are very constrained where there is a small set of Lie algebra representations that

* Corresponding author.
E-mail address: Marcelo@QuantumGravityResearch.org (M. Amaral).

[1] Note that the $SU(3)$ group can be connected both with gauge field as with fermions. The gauge fields are usually modeled in the adjoint representation and the fermions in the fundamental representation. In our case one can expect that if we go back from the spin foam state sum transition amplitudes to the action level, we should get actions for both the gauge fields and fermions.

https://doi.org/10.1016/j.physo.2021.100098
Received 27 July 2021; Accepted 22 December 2021
Available online 11 January 2022
2666-0326/

interact, and the syntax of its fusion rules works as a glue, indicating topological order [13,14]. With a tetrahedron building block the problem is translated to an issue of how to tile the space, where we will be mainly concerned with 3-dimensional space, which can be linked with the Fibonacci anyonic fusion Hilbert space, which is one of our motivations to choose the specific fifth root of unity deformation of Lie algebras. In this way we propose the fifth root of unity deformation as our postulate for quantization of geometry in 3D, which also simplifies the computation of transition amplitudes and observables.

This paper is organized as follows: in Section 2 we present the fifth root of unity quantization postulate for geometry in 3D and its associated Fibonacci fusion Hilbert space interpretation. In Section 3 we discuss the coupling of the model with internal $SU(3)$ symmetries and suggest a natural extension to the larger $SU(N)$, G_2, and E_8, with the same fifth root of unity deformation. In this constrained framework, we are able to explicitly calculate some observables and the amplitudes — our main result. We also discuss the polytope interpretation of the amplitudes. We present our conclusions in Section 4. In Appendix A we review the usual concept of 3D spin foam quantum gravity, and present its modified topological regularized version based on the Turaev and Viro model. In Appendix B we present a review of the grand unification physics program.

2. 3D Spin foam and quantum groups at the fifth root of unity

We review the usual spin foam models and its q-deformation regularization in Appendix A. Here we propose to derive the large spin transition amplitude discussed in the appendix from the direct quantization of geometry, in particular a quantum building block, a tetrahedron, following the notion of quantum tetrahedrons [15] as a quantization postulate for geometry. It is well known that in 3D gravity only has topological degrees of freedom. We postulate the topological fifth root of unity symmetry, to be discussed below, as the quantization postulate in 3D and discuss that it implies a topological quantum computer picture of pre-spacetime.

2.1. The quantum tetrahedron with topological symmetry

The quantization of one tetrahedron allows us to define and address the quantization of geometric quantities like lengths, areas and volumes. Yet the usual quantization with $SU(2)$ symmetry is much too general, allowing divergences for these geometric quantities. A kind of regularization can be done by implementing restrictions on the representation theory of Lie algebras — the usual deformation of the classical algebra with a complex root of unity parameter.

Let us discuss a specific model implementation. Most of the geometric quantities of interest such as lengths, areas and volumes can be described in a simple, unifying form from the geometry of the 3-simplex, the tetrahedron. The tetrahedron can be described by its 4 (outgoing) normals, vectors $\mathbf{L}_a$ in its four triangular faces, $a = 1, 2, 3, 4$, subject to the closure constraint

$$\mathbf{C} = \sum_{a=1}^{4} \mathbf{L}_a = 0. \tag{1}$$

All geometric properties of the tetrahedron can be derived from the normals and must be invariant under a common $SO(3)$ rotation of the tetrahedron. For example, the area of face a is given by $A_a = |\mathbf{L}_a|$ and the volume is defined by $V^2 = \frac{2}{9}\left(\mathbf{L}_1 \times \mathbf{L}_2\right) \cdot \mathbf{L}_3$. The proposed quantizing postulate is a quantum deformation of Eq. (A.2). Eq. (A.2) is the $SU(2)$ algebra implied by the 3 dimensional rotational symmetry, where the normals are promoted to operators L_a and identified with the generators of the algebra L_a^i ($i = 1, 2, 3$). We first write the classical algebra in terms of Cartan generators and root vectors, which are the usual ladder operators of $SU(2)$, then choose the Cartan generator $h_a = L_a^3$ and the root vectors $L_a^{\pm\alpha} = L_a^1 \pm \alpha i L_a^2$, where for $SU(2)$, $\alpha = 1$, and we have

$$\begin{aligned} \left[h_a, L_b^{\pm}\right] &= \pm\beta\delta_{ab}L_a^{\pm} \\ \left[L_a^{+}, L_b^{-}\right] &= 2\beta\delta_{ab}h_a, \end{aligned} \tag{2}$$

where β has the dimension of area. The usual Casimir invariant is $L_a^i L_a^i = L_a^+ L_a^- + h_a\left(h_a + \beta\right)$, commuting with each element of the algebra, and has eigenvalues[2] $\beta^2 j_a(j_a+1)$, $j_a \in 0, \frac{1}{2}, 1, \frac{3}{2}, 2, \ldots$, which gives a quantization of area $A_a = \beta\sqrt{j_a(j_a+1)}$ for a triangular face or $A_{j_{an}} = \beta\sum_n \sqrt{j_{an}(j_{an}+1)}$ for an arbitrary surface punctured by N punctures $n_1, \ldots, N$. As discussed in the Appendix A, there are no restrictions on the flow of spin representations in this case, suggesting we should implement a more fundamental topological symmetry. So we apply the $SU(2)_q$ deformation at the fifth root of unity $q = e^{\frac{2\pi i}{r}}$, with $r = 5$ (from now on let us call it $SU(2)_q^5$), which affects the Cartan generator in the second term and constitutes essentially a quantization postulate for geometry (see [16] for additional motivation):

$$\begin{aligned} \left[h_a, L_b^{\pm}\right] &= \pm\delta_{ab}L_a^{\pm} \\ \left[L_a^{+}, L_b^{-}\right] &= 2\delta_{ab}\left[2h_a\right]_q, \end{aligned} \tag{3}$$

with the q number $[x]_q$ defined by

$$[x]_q = \frac{q^{\frac{x}{2}} - q^{-\frac{x}{2}}}{q^{\frac{1}{2}} - q^{-\frac{1}{2}}} = \frac{sin\left(\frac{\pi}{5}x\right)}{sin\left(\frac{\pi}{5}\right)} \tag{4}$$

or writing the Cartan generator, $\mathcal{J}_a = q^{h_a}$:

$$\begin{aligned} \mathcal{J}_a L_b^{\pm} \mathcal{J}_a^{-1} &= q^{\pm 1} L_b^{\pm} \\ \left[L_a^{+}, L_b^{-}\right] &= 2\delta_{ab}\frac{\mathcal{J}_a - \mathcal{J}_a^{-1}}{q - q^{-1}} \end{aligned} \tag{5}$$

For this deformation to be dimensionally consistent, we start with everything adimensional and there is no need a priori for β. There is a notion of scale incorporated in the deformation parameter, $r = \frac{l_c}{l_p}$, with r an integer and the large scale l_c given in units of the underlying scale l_p. This representation theory is as well understood as that of $SU(2)$. There are 3 independent Casimir invariants for each face $C_{aq} = L_a^+ L_a^- + \left[h_a\right]_q\left[h_a + 1\right]_q$, $X_a = (L_a^+)^5$ and $Y_a = (L_a^-)^5$. When X_a and Y_a have zero eigenvalues for all vectors in the linear vector space carrying the irreducible representation, the representations have classical analogs, and can be constructed by specializing from the general values of q to the specific root of unity. In this case the spin quantum numbers that label the representations of $SU(2)_q$ are constrained to $j_a \le \frac{3}{2}$, and are related to the Casimir C_{aq} of eigenvalues $[j_a]_q[(j_a+1)]_q$. In this way the area spectrum interpretation

$$A_a = \sqrt{[j_a]_q[(j_a+1)]_q} \tag{6}$$

is not immediate and a scale should emerge in an appropriate limit.

The vertex amplitude is naturally given by the specialization of Eq. (A.6) to $SU(2)_q^5$ symmetry defined by the Hilbert space of the tensor product of 4 representations at the vertex $H_{j_{q1}} \times H_{j_{q2}} \times H_{j_{q3}} \times H_{j_{q4}}$, and it is a function of the representations on the 6 boundary faces defined by this vertex

$$W^5_{\triangle_1}(j_{lv}) = (-1)^{j_v}\left\{\begin{array}{ccc} j_1 & j_2 & j_3 \\ j_4 & j_5 & j_6 \end{array}\right\}_5, \tag{7}$$

with $j_{lv} = j_1, \ldots, j_6$ and the index 5 representing the $SU(2)_q^5$ deformation. The q-deformed 6-j symbols, $\{6j\}_5$, for the 4096 combinations of j's in $0, 1/2, 1, 3/2$, are all null except for a small set of combinations, which can be computed from Eq. (18) restricted to the $SU(2)$ case and takes on only seven values: $\{0, \pm 1, \pm\varphi, \pm\sqrt{\varphi}\}$, where $\varphi = \frac{\sqrt{5}-1}{2} = \phi^{-1}$, with $\phi = \frac{\sqrt{5}+1}{2} = 1.618\ldots$, the golden ratio.

[2] Splitting the constant with dimension of area $j_a \to \beta j_a$.

More generally, this kind of amplitude is independent of the triangulation, and gives a topological invariant as described in the Turaev and Viro model [17], which means that it does not depend on the triangulation inside the 3 manifold, but depends only on the edge values and on the topology of the triangulated 3 manifold (the number of punctures on the boundary 2-sphere). Exploiting the possibility to build invariants by fixing the representations labels on the edges we can consider networks of these topological amplitudes, which act as building blocks for decomposing a higher dimensional tensor product space, which we will motivate more in the next section. For example, we can consider amplitudes, functions of representations on boundary faces of edges for closed loops along the 3 dimensional spin foam

$$W_c(j_{lc}) = \mathcal{N}_q \sum_{j_f|j_{lc}} \prod_f (-1)^{j_f} d_q(j_f) \prod_v W^5_{\triangle_1}(j_{lv}), \tag{8}$$

where c is a closed loop across the 3 dimensional triangulation and $j_{lc} = j_1, \ldots, j_n$ are the representations on the boundary faces of the n edges contained in c. The sum $\sum_{j_f|j_{lc}}$ is taken while maintaining those boundary faces of the edges of c fixed. The notation with the sum and products in Eq. (8) is to indicate that one needs to use all possible configurations allowed.

2.2. Motivation for the fifth root: Fibonacci fusion Hilbert space

We now consider the topological data of $SU(2)^5_q$. The admissible spin representations are $j = 0, \frac{1}{2}, 1, \frac{3}{2}$, and their quantum dimension are given by

$$d^q_j = sin\left(\frac{\pi(2j+1)}{5}\right)/sin\left(\frac{\pi}{5}\right). \tag{9}$$

The composition of representations follows the following fusion rules:

$$\begin{aligned} 0 \otimes j &= j \\ \frac{3}{2} \otimes j &= \frac{3}{2} - j \\ \frac{1}{2} \otimes \frac{1}{2} &= 0 \oplus 1 \\ \frac{1}{2} \otimes 1 &= \frac{1}{2} \oplus \frac{3}{2} \\ 1 \otimes 1 &= 0 \oplus 1. \end{aligned} \tag{10}$$

Remember that a segment of the triangulation is dual to a face on the dual 2-complex where there is attached a representation of $SU(2)^5_q$. Fundamentally there are 2 states on the segments, one with quantum dimension 1 and one with quantum dimension ϕ, and we have a notion of a 2-dimensional fusion Hilbert space [13,14] as the superposition of these 2 states. The space $H_{j_{q1}} \times H_{j_{q2}} \times H_{j_{q3}}$ is in this way 3-dimensional and is related to the triangular faces. The tetrahedron $H_{j_{q1}} \times H_{j_{q2}} \times H_{j_{q3}} \times H_{j_{q4}}$ is 5 dimensional. The dimensions grow with the increasing number of representations, following the well known Fibonacci sequence, which gives the name of Fibonacci anyons for the representations of the $SU(2)^5_q$ symmetry in context of topological phases of matter and quantum computing fields of researches. In this language the $A_v = W^5_{\triangle_1}(j_{lv})$ building block amplitude is just the known F symbol that appears in those anyonic models [13,14]. The partition function is about gluing these A_v amplitudes, which makes sense from the point of view of quantum computation. An important result in the field of quantum computation is that a higher dimensional Hilbert space can be decomposed into a network of qubits and 2-level quantum gates [18], and that with at least 3 Fibonacci anyon representations, one can implement the qubits, where the braids of these anyons can approximate any 2-level quantum gate, making Fibonacci anyons a sufficient substrate for universal quantum computation [13]. It has been shown that anyons described by Chern–Simons theory at some root of unity r can give rise to universal quantum computation for $r = 5$ or $r > 7$ [13,19]. So $Z_q(nj)$ of n "anyon states", for large n, can be understood as a topological quantum computer but described by the network of the building block amplitudes $A_v = W^5_{\triangle_1}(j_{lv})$. The dual 2-complex of the quantum tetrahedron is made of one vertex in the bulk and 4 nodes on the triangular boundary faces of the triangulation. The quantum tetrahedron carries 4 anyonic charges, the 4-tensor product of the $H_{j_{qi}}$ above, implemented by A_v. The extension of the topological data from $SU(2)^5_q$ to $SU(N)^r_q$ is presented in the next section.

Table 1
Fusion rules of $SU(3)^5_q$.

$\otimes$	(10)	(01)	(20)	(02)	(11)
(10)	(01) ⊕ (20)				
(01)	(00) ⊕ (11)	(10) ⊕ (02)			
(20)	(11)	(10)	(02)		
(02)	(01)	(11)	(00)	(20)	
(11)	(01) ⊕ (02)	(01) ⊕ (20)	(01)	(10)	(00) ⊕ (11)

3. Fermionic cycles and gauge symmetry unification

The natural symmetry for the quantum tetrahedron, as discussed in Section 2.1, is the spatial rotations $SO(3)$ in 3D, implemented by the covering group $SU(2)$, and hence its fifth-root-of-unity deformation. But the generalization of $SU(2) = A_1$ in the Weyl–Cartan or Chevalley basis to the higher dimensional simple Lie algebras, Eq. (B.6), indicates that we can incorporate the so called internal symmetry or charge space in the same way. The simplest way is to consider the symmetry $SU(2) \times G$, with G one of the higher dimensional simple Lie algebras [20]. Because of the importance of A_1 the natural first candidate is $G = A_2 = SU(3)$. Following this, we will also define an extension of the topological data from $SU(2)^5_q$ to $SU(N)^r_q$. To get onto multi-dimensional Fibonacci-like anyonic representations and fulfill the quantizing postulate Eq. (3), we will further restrict r to be a multiple of 5 larger than N. Examples useful for gauge unification that have the Fibonacci fusion Hilbert space structure are $SU(3)^5_q$, $SU(4)^5_q$, $SU(5)^{10}_q$, $SU(8)^{10}_q$ and $SU(9)^{10}_q$. This allows us to address the higher dimensional A_4, whose Coxeter—Dynkin diagram splits into two copies of A_2, and E_8, the largest exceptional Lie algebra, which has four A_2 building blocks as shown in Fig. B.3. As is well known, $A_4 = SU(5)$ and E_8 are very important for unification physics. We will also discuss the exceptional Lie algebra G_2, which contains $SU(3)$ and has a fifth-root deformation with Fibonacci fusion rules.

3.1. Spin foam at the fifth root of unity with fermionic cycles and gauge symmetry

Following [21,22], the deformation of the $SU(3)$ algebra ($SU(N)$ in general) Eq. (B.6) at the fifth root of unity is given by:

$$\begin{aligned} \left[h_i, h_j\right] &= 0 \\ \left[h_i, L^\pm_j\right] &= \pm C_{ij} L^\pm_j \\ \left[L^+_i, L^-_j\right] &= \delta_{ij}\left[2h_i\right]_q, \\ \left(L^\pm_i\right)^2 L^\pm_j - [2]_q L^\pm_i L^\pm_j L^\pm_i + L^\pm_j \left(L^\pm_i\right)^2 &= 0, \qquad i \neq j \end{aligned} \tag{11}$$

which reduces to Eq. (B.6) when q goes to 1. From Eq. (4), $[2]_q = \phi$ in our case.

$SU(3)$ has two Cartan generators and as in the case of $SU(2)$ we label its representations by the eigenvalues of the Cartan generators. So the representations are labeled by 2 Dynkin labels $g = (p_1 p_2)$ in the notation introduced above for their associated "polytopes", or in a more compact form by its classical dimension 1, 3, $\bar{3}$, 6, $\bar{6}$, 8 and so on. For $SU(3)^5_q$ the fusion rules are limited to the lower dimensional representations $1 = (00)$, $3 = (10)$, $\bar{3} = (01)$, $6 = (20)$, $\bar{6} = (02)$ and $8 = (11)$. The fusion rules are given by $(00) \otimes (p_1 p_2) = (p_1 p_2)$ and Table 1.

To compute for general $SU(N)_q$ the quantum dimensions $d_q(g)$, which will be the edge amplitudes, the spin number j of Eq. (9), for a specific representation, is extended to a Dynkin label $(p_1,\dots,p_{N-1})$ describing the highest weight of the representation. For general N, $d_q(p_1,\dots,p_{N-1})$ will be computed by the following algorithm: a Young diagram is drawn for the Dynkin label as a set of N left-justified rows of p_1, p_2, $\dots p_{N-1}$ cells, from top to bottom. If $p_{N-1}>0$ there exists a minimal M index, $0<M<N$ such that $p_{M+1}=0$, and we draw only M rows, otherwise we set $M=N-1$. Accumulating its value from the right to the left, we create a partition numbering the length of successive rows in the Young diagram. The Young diagram can be filled by numbers beginning at the top-left by an integer between 1 and N, non increasing from left to right and strictly decreasing from top to bottom, which enable to compute the number of elements corresponding to different Young tableaux. This is the dimension of the representation. It can be expressed by the Weyl dimension formula as the ratio: the numerator is the product of the number in each box of a tableau beginning with N at the top-left, strictly increasing to the left and strictly decreasing to the bottom, while the denominator is the product of the hook number of each box, where the hook number of any box is the number of boxes met by a hook beginning at the right of the row, tracing horizontally to the box, then tracing vertically to the bottom. Because the numerator will vanish if there are more than $N-1$ rows, the number of rows is limited. For the quantum deformation, the same Weyl formula is applied but the integers in each box are now quantum integers defined by Eq. (4), where $[r]_q=0$. Therefore the Young diagram cannot have more than $r-N$ columns, which sets a cut-off for the number of representations. For $N=3$ the quantum dimension is given by

$$d_q(p_1,p_2)=[p_1+1]_q[p_2+1]_q[p_1+p_2+2]_q/[2]_q. \tag{12}$$

The quantum dimension $d_q(g)$ for $g=(00),(20),(02)$ is $d_q(g)=1$ and for $g=(10),(01),(11)$ is $d_q(g)=\phi$. For general N the quantum dimension is given by [21]

$$d_q(p_1,p_2,..,p_{N-1})=\prod_{j=1}^{N-1}\prod_{k=0}^{N-1-j}\frac{[\sum_{l=1}^{j}1+p_{k+l}]_q}{[j]_q} \tag{13}$$

Alternatively, we can use the general formula from which Eq. (9) is derived, a deformation of the Weyl dimension formula to

$$d_q(g)=\prod_{\alpha}\frac{\left[(\omega_g+\rho,\alpha)\right]_q}{[(\rho,\alpha)]_q}, \tag{14}$$

where $\omega_g=(p_1,\dots,p_{N-1})$, the highest weight describing the irreducible representation, is given by Eq. (B.3). The vector ρ is half the sum of positive roots $\rho=\frac{1}{2}\sum_\alpha\alpha$ and α represent the positive roots. For $SU(2)$ there are only one positive root $\alpha_1=(1,-1)$ and the fundamental weight is given by $\omega_1=(1/2,-1/2)$, so $\rho=(1/2,-1/2)$ and $\omega_g=p_1\omega_1=2j\omega_1$ and Eq. (14) reduces to Eq. (9). For $N=3$, from Eq. (B.5), the third positive root is $\alpha_3=(1,0,-1)$, $\rho=(1,0,-1)$ and $\omega_g=p_1\omega_1+p_2\omega_2$. Thus the quantum dimension reduces to Eq. (12).

We now compute the $\{6g\}^5$ symbols associated with a tetrahedron edge decoration by representations of the $g=SU(3)_q^5$ algebra, which can be generalized to $g=SU(N)_q^r$. The computation of the amplitudes $\{6g\}^5$ for $SU(N)_q$ can always be done case by case as in [22] but we have adapted the formulas from [23], replacing spins by a suitable projection of the highest weight vectors in the case of multiplicity-free quantum $\{6g\}$-symbols, where we will deal with representations (10), (01) and (00) for $g=SU(3)_q^5$. On the decomposition of $(11)\otimes(11)$, we already have to deal with multiplicities [22]. This projection operator depends on the algebra:

$$(w_1w_2...w_{N-1})'=Pr(N,(w_1w_2...w_{N-1})) \tag{15}$$

and in our multiplicity-free case is given by

$$(w_g)'=\frac{1}{2}\sum_\alpha(\omega_g,\alpha), \tag{16}$$

where again $\omega_g=(p_1,\dots,p_{N-1})$, the highest weight describing the irreducible representation, and α represent the positive roots. In the case of $SU(2)$ it gives the usual half integers j and in the case of $SU(3)$ it gives p_1+p_2. So we have

$$\begin{aligned}\Delta'(abc)=&([(-a+b+c)']![(a-b+c)']![(a+b-c)']!)^{1/2}\\ &\times([(a+b+c)'+1]!)^{-1/2}\end{aligned} \tag{17}$$

where $[m]_q!=\prod_{n=1}^m[n]_q$ and

$$\begin{aligned}\{6g\}^5(abcdef)&=\left\{\begin{array}{ccc}a&b&e\\d&c&f\end{array}\right\}_q=\\&=\Delta'(abe)\Delta'(acf)\Delta'(ced)\Delta'(dbf)\sum_z\frac{\nu}{\delta},\end{aligned} \tag{18}$$

where z is an integer vector of $\mathbb{N}^{(N-1)}$ inside the polytope where the expression is not null, and ν and δ are

$$\begin{aligned}\nu=&(-1)^{z'}[(z)'+1]!\{[(z-a-b-e)']![(z-a-c-f)']!\\&\times[(z-b-d-f)']![(z-d-c-e)']!\}^{-1}\end{aligned} \tag{19}$$

$$\delta=[(a+b+c+d-z)']![(a+e+f+d-z)']![(e+b+c+f-z)']!. \tag{20}$$

Finally, the F-symbol $((F_c^{abd})_{ef})$ is given from:

$$\left\{\begin{array}{ccc}a&b&e\\d&c&f\end{array}\right\}_q=(-1)^{(a+b+c+d+e+f)'}(d_q^{e'}d_q^{f'})^{-1/2}(F_c^{abd})_{ef}, \tag{21}$$

where $d_q^{e'}$ is the quantum dimension of the representation of highest weight e. The fusion matrix $\left(\left[\begin{array}{cc}a&b\\d&c\end{array}\right]\right)$ is obtained from:

$$(F_c^{abd})_{ef}=a_{ef}\left[\begin{array}{cc}a&b\\d&c\end{array}\right]. \tag{22}$$

For $N=3$, we can use either the F-symbols from [22] or the fusion matrix from [24]. The following are two examples showing the coherence of our formulas (21) and (22) with (18) and with some results given in [21–24]:

$$\begin{aligned}\left\{\begin{array}{ccc}01&10&00\\01&01&00\end{array}\right\}_q&=(-1)^4(d_q^{00'}d_q^{00'})^{-1/2}(F_{01}^{01\ 10\ 01})_{00\ 00}\\&=(1)^{-1/2}(F_{\bar{3}}^{\bar{3}\ 3\ \bar{3}})_{1\ 1}=(F_3^{3\ \bar{3}\ 3})_{1\ 1}\\&=a_{00\ 00}\left[\begin{array}{cc}01&10\\01&01\end{array}\right]=[3]_q^{-1}\end{aligned} \tag{23}$$

and

$$\begin{aligned}\left\{\begin{array}{ccc}10&01&00\\01&01&10\end{array}\right\}_q&=(-1)^5(d_q^{00'}d_q^{10'})^{-1/2}(F_{01}^{10\ 01\ 01})_{00\ 10}\\&=(-1)(\phi)^{-1/2}(F_{\bar{3}}^{3\ \bar{3}\ \bar{3}})_{1\ 1}=-(\phi)^{-1/2}(F_3^{\bar{3}\ 3\ 3})_{1\ 3}\\&=-(\phi)^{-1/2}a_{00\ 10}\left[\begin{array}{cc}10&01\\01&01\end{array}\right]=-[3]_q^{-1}.\end{aligned} \tag{24}$$

A complete algorithm to compute $SU(4)$ Clebsch–Gordan coefficients is available in [25]; it can be extended to compute the 6j-symbols of $SU(4)$ for all representations. The algorithm may be extended to higher dimensions and deformed by a procedure replacing factorials by quantum factorials and using projected weights. The Fibonacci anyons in $g=SU(4)_q^5$ will be restricted to only 4 representations, the fundamental (000), the symmetric (100), its conjugate antisymmetric (001) and the antisymmetric (010). Their respective quantum dimensions are $[1]_q$, $[1]_q$, $[4]_q$ and $[4]_q[3]_q/[2]_q$. For $r=5$ these quantum numbers are all equal to 1, therefore this is adapted to decorate a graph with only one edge length, while $SU(2)_q^5$ and $SU(3)_q^5$ decorate graphs with two edge lengths. The cut-off in the number of representations comes from the fact that $r-N$ is small. The next representations, which would be of interest for a higher r, are the symmetric (200), cut-off at $r=5$, and the symmetric (300), cut-off at $r=6$. The Young tableau of (200) is a row with two boxes. In the dimension formula, the numerator is the product of the two boxes, where the leftmost has the quantum integer $[N]$ and each one at its right increases by one, so the right one is $[N+1]=[r]=0$, which cancels this representation.

There is no representation in $SU(5)^5_q$, so we study $SU(5)^{10}_q$, which is quite rich. When N increases to meet $r-1$, the structure simplifies and there are only 9 antisymmetric representations in $SU(9)^{10}_q$: $(0^8),(1\ 0^7),(0^1\ 1\ 0^6),(0^2\ 1\ 0^5)...(0^6\ 1\ 0^1)$ and $(0^7\ 1)$. They will be the bricks for the branching of E^{10}_{8q} to A^{10}_{8q}, which is a subject of our ongoing work.

3.2. Observables

The observables of interest, to be motivated with explicit examples below, can be calculated from the generalization of Eq. (8) to include fermions, which are defined as closed oriented cycles on the dual 2-complex $\triangle^*$, with $SU(3)^5_q$ representations on its edges. These fixed states can be interpreted as observables [26]. The observable of interest is

$$O_{\triangle_{4^l}}(g_c,j_{lc}) = \mathcal{N}_q \sum_{\{c\}} \sum_{j_f|j_{lc}} \prod_f (-1)^{j_f} d_q(j_f) \prod_v W^5_{\triangle_1}(j_{lv}) \prod_c \left(\prod_{e\in c} (-1)^o d_q(g_e) \right) \{6g\}^5 \tag{25}$$

where o gives a sign due to the match or mismatch of the orientations of $\triangle^*$ and the cycles $\{c\}$. In this sense the cycles are fermionic — there cannot be more than one cycle on one edge with the same orientation relative to the orientation of $\triangle^*$. The maximum is two cycles on one edge with opposite orientation, which constrains the possible cycles. Each edge on a cycle c has one amplitude given by the quantum dimension $d_q(g_e)$ of the $SU(3)^5_q$ representation g on it. The $\triangle_{4^l}$ is a triangulation at level l, which we can explain with examples:

- The level $l=0$ triangulation is just one tetrahedron in $\triangle$ and one vertex inside the boundary tetrahedron.
- At the level $l=1$ triangulation we start with one tetrahedron and connect its center with its 4 points, making four new tetrahedrons. Then we take the dual 2-complex in the usual way by inserting a vertex inside each tetrahedron and connecting them. (See Fig. A.2).
- At the level $l=2$ triangulation, our space is divided into 16 tetrahedrons. The dual 2-complex in the bulk has 16 vertices at their centers. (See Fig. 1). And so on.

The observables $O_{\triangle_{4^l}}(g_c,j_{lc})$ are functions of the $SU(2)^5_q$ j_{lc} representations on the boundary faces of $\triangle^*$ and $SU(3)^5_q$ g_c on the edges of the closed cycles. To correctly assign the $\{6g\}^5$ on the network, we need to consistently choose the cycles and give consideration on how to constraint our cycles of interest. Let us discuss this level by level.

The level $l=0$ observables:

The level $l=0$ has no bulk edges and so there are only pure topological (gravitational) observables, Eq. (7).

The level $l=1$ observables and its $\{6g\}^5$:

We note that the usual observables at $l=0$ above, $W^5_{\triangle_1}(j_{lv})$, are functions of the six representations on the six boundary faces of the 2-complex, or equivalently on the segments (edges of the tetrahedron) of the triangulation. We can then associate a "polytope" of $SU(2)$ to these representations; they are the edges of the tetrahedron, and the building block is the Delone polytope, the edge of $p=1$ of the (1) representation. The only representation that does not have this interpretation is the scalar (0), which can work as "dummy" indices in the $W^5_{\triangle_1}(j_{lv})$. This suggests that the observables of interest for $SU(3)^5_q$ are the ones that have a "polytope" interpretation in $SU(3)^5_q$ so that the $\{6g\}^5$ would be a function of these "polytopes". In particular, these would be the Delone polytopes, (10) or (01), and, when necessary, a "dummy" index with the (00) representation to complete the $\{6g\}^5$ input representations.

Immediately we note that, consistently, each edge of a cycle on $\triangle^*$ is dual to a triangle of the $\triangle$ and so it can have a representation $g=(10),(01)$ or $g=(00)$ sitting on it. From Fig. A.2 let us label the representations:

- $SU(2)^5_q$ on the faces of $\triangle^*$, using the numbers labeling the vertices: $j_1=j_{12}$, $j_2=j_{13}$, $j_3=j_{14}$, $j_4=j_{23}$, $j_5=j_{24}$, $j_6=j_{34}$, $j_7=j_{123}$, $j_8=j_{124}$, $j_9=j_{134}$, $j_{10}=j_{234}$.
- And for $SU(3)^5_q$ on the edges from the 4 internal vertices: $g_1=g_{12}$, $g_2=g_{13}$, $g_3=g_{14}$, $g_4=g_{23}$, $g_5=g_{24}$, $g_6=g_{34}$.

So, for the observable $O_{\triangle_4}(g_{1...6},j_{1...6})$ the $\{6g\}^5$ is naturally associated with the bulk tetrahedron with vertices 1,2,3,4, coupling six g representations on its six edges. So the set of allowed cycles $\{c\}$ are the ones covering this tetrahedron, and this can be done with 4 triangular cycles. Note that any configuration with all (01) or (10), e.g. $g_{1...6}=((10),(01),(10),(10),(10),(01))$, gives $\{6g\}^5=0$. But by inserting the representation (00) we can have non-zero $\{6g\}^5$ and the observables can be computed, as for example for $g_{1...6}=((01),(10),(01),(01),(00),(00))$, which gives, from Eq. (23), $\{6g\}^5=\phi^{-1}$. In this case, for the amplitude $\{6g\}^5$ we are using the fundamental (10) and anti-fundamental (01) representations which compose the Voronoi polytope of $SU(3)$.

One example of an interesting observable, which can be interpreted as a coupling interaction of the $SU(2)^5_q$ and $SU(3)^5_q$ representations, is defined in the following way. First we choose an orientation on $\triangle^*$ to be given by one incoming edge from the boundary to vertex 4, then to vertices 1, 2 and 3. From 3, the oriented edges go to 1, 2 and from 1, 2 they go out (see Fig. A.2). The cycle c_1 is 123, c_2 is 142, c_3 is 134 and c_4 is 243. There is only one other option of cycles, which is the one with the inversion of orientation of all 4 cycles. For $g_{1...6}=((10),(01),(01),(01),(00),(10))$ fixed, from Eq. (24), $\{6g\}^5=-\phi^{-1}$, imposing consistency of both representations on $\triangle$ (where, for example, a $g_1=(01)$ fixes $j_1=1/2$ $(p=1,\ j=2p)$) leads to $j_{1...10}=(\frac{1}{2},\frac{1}{2},\frac{1}{2},0,0,0,0,\frac{1}{2},0,\frac{1}{2})$. Thus, working with the unnormalized amplitudes, we have

$$\begin{aligned} O_{\triangle_4}(g_{1...6},j_{1...10}) = {} & (-1)^{j_1}...(-1)^{j_{10}} d_q(j_1)...d_q(j_{10}) W^5_{\triangle_1}(j_{v_1})...W^5_{\triangle_1}(j_{v_4}) \\ & \left(-d_q(g_1)d_q(g_2)d_q(g_4)\right)\left(d_q(g_1)d_q(g_3)d_q(g_5)\right) \\ & \left(d_q(g_2)d_q(g_6)d_q(g_3)\right)\left(-d_q(g_6)d_q(g_4)d_q(g_5)\right) \\ & \{g_1...g_6\}^5. \end{aligned} \tag{26}$$

Note that in this example all internal j's are fixed by fixing the g's, and so we could first have fixed all the 10 j's, which gives a topological invariant observable of $SU(2)^5_q$ [26], and the g's can be interpreted as emergent properties of the network.

The level $l=2$ observables and its $\{6g\}^5$:

Now we have 4 tetrahedrons similar to the ones on $l=1$. They are connected to form 4 hexagonal cycles (see Fig. 1, where internal vertices are labeled with positive integers and external points with negative integers): $c_1=\{7, 14, 15, 11, 10, 6\}$, $c_2=\{6, 10, 12, 19, 18, 8\}$, $c_3=\{8, 18, 20, 16, 14, 7\}$, $c_4=\{11, 15, 16, 20, 19, 12\}$, where c_n is a hexagonal face (an irregular hexagon alternating short and long links), viewed from an outside point $-n$. Along each of these cycles, the 3 long edges are shared with short cycles completed by a vertex making a dual tetrahedron. For c_1: $c_{1.2}=\{15, 14, 16 \text{ or } 13\}$, $c_{1.3}=\{10, 11, 12 \text{ or } 9\}$, $c_{1.4}=\{7, 6, 8 \text{ or } 5\}$. The link $c_{1.2}$ is shared between c_1, c_3 and c_4, therefore $c_{1.2}=c_{3.2}=c_{4.2}$. The link $c_{1.3}$ is shared between c_1, c_2 and c_4, so $c_{1.3}=c_{2.3}=c_{4.3}$. The link $c_{1.4}$ is shared between c_1, c_2 and c_3, so $c_{1.4}=c_{2.4}=c_{3.4}$. The last short cycles are $c_{2.1}=c_{3.1}=c_{4.1}=\{18, 19, 20 \text{ or } 17\}$. All four short cycles extended as tetrahedrons cover all the 16 level $l=2$ vertices (centers dual to the $l=2$ tetrahedrons), here indexed from 5 to 20.

Emerging $\{6g\}^5$ symbols:

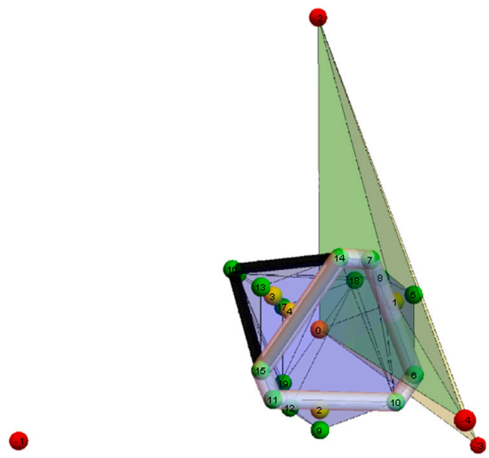

Fig. 1. This figure shows the hexagonal cycle c_1 in white and the triangular cycle $c_{1.2}$ in black. They share the link l(14–15).

- for a tetrahedron $\{6g\}^5(c1.2) = \left\{ \begin{array}{ccc} g_{15-14} & g_{14-16} & g_{16-15} \\ g_{15-13} & g_{14-13} & g_{16-13} \end{array} \right\}_q$;
- for a hexagon $\{6g\}^5(c1) = \left\{ \begin{array}{ccc} g_{7-14} & g_{14-15} & g_{15-11} \\ g_{11-10} & g_{10-6} & g_{6-7} \end{array} \right\}_q$.

(See Fig. 1).

3.3. Unification physics from the exceptional Lie algebras

Let us consider the lowest dimensional exceptional Lie algebra, G_2, at the fifth root of unity - $G^5_{2_q}$. G_2, like $SU(3)$, is of rank 2, and is the only exceptional one for which a fifth-root quantum deformation is possible. The generalization of Eq. (11) to the exceptional Lie algebras has only 2 equations changed, namely [21,22],

$$\left[L_i^+, L_j^-\right] = \delta_{ij}\left[2h_i\right]_{q_i},$$

$$\sum_{s=0}^{1-C_{ij}} (-1)^s \left(\begin{array}{c} 1-C_{ij} \\ s \end{array} \right)_{q_i} \left(L_i^\pm\right)^{1-C_{ij}-s} L_j^\pm \left(L_i^\pm\right)^s = 0, \qquad i \neq j \quad (27)$$

where $C = \left(\begin{array}{cc} 2 & -3 \\ -1 & 2 \end{array} \right)$ and $q_i = q^{\frac{1}{t_i}}$, with $t_i = \frac{2}{(\alpha_i, \alpha_i)}$, which gives for $G^5_{2_q}$, $t_1 = 1$ and $t_2 = 3$. The q_i binomials are $\left(\begin{array}{c} m \\ n \end{array} \right)_{q_i} = \frac{[m]_{q_i}!}{[n]_{q_i}![m-n]_{q_i}!}$, with $[m]_{q_i}! = \prod_{n=1}^m [n]_{q_i}$ and $[n]_{q_i}$ given by Eq. (4) using q_i. There are only 2 representations in the fusion rules, the 1 dimensional $1 = (00)$ and the 7 dimensional, $7 = (01)$[3]. The only non trivial fusion rule is

$$(01) \otimes (01) = (00) \oplus (01), \quad (28)$$

which is the well known Fibonacci (anyon) fusion rule. The quantum dimensions, which are the amplitudes on the edges of the $\triangle^*$, are $d_q^{(00)} = 1$ and $d_q^{(01)} = \phi$. For the $\{6g\}^5$ amplitudes for $G^5_{2_q}$ there are 64 possibles ones but only 15 are not null, which constrains the available observables. They are given in [22]. It is therefore easy to compute observables for $G^5_{2_q}$ using Eq. (25) and following the procedure of previous sections. In the first levels of the triangulation, however, we find no polytope interpretation, which would be a hexagon with a point in the center, on the triangulation. This leads us to suggest that the exceptional Lie algebras work as a container for the lower dimensional Lie algebras, $SU(2)$ and $SU(3)$, which are in fact the gauge symmetries. Note that the fusion rule of $\{6g\}^5$ contains only the representations that appear in the observable Eq. (26), because the 7 of G_2 contains the (10), (01) and (00) of $SU(3)$. This gives a role to G_2 as the one that unifies those lower dimensional gauge symmetries.

With $G^5_{2_q}$ having only one non-trivial fusion rule, the generalization to higher dimensional Lie algebras may best be done with the tenth root of unity. Another option is that our observables already capture information of higher dimension through projection. This can be seen from the Coxeter—Dynkin diagram of $SU(5)$ and E_8. See for example the magic star projection of E_8 to 2D [27].

4. Conclusions

In this paper we have presented quantum gravity observables coupling internal gauge symmetry with spacetime symmetry in a spin foam model. We note that in usual spin foam or state sum models in 3D, there are 2D states, whose evolution is described by 3D transition amplitudes. In this paper we presented a Wilson lattice gauge theory perspective where fermionic observables are cycles that go through the 3D foam. This fixes a notion of 3D states for the 3D theory. Thus the whole discussion of transition amplitudes in 3D, which one might ordinarily think of as being about dynamics, is in fact more about the kinematics of quantum gravity. Note that the kinematical space of 3D spin foam theory is the same as for 4D, i.e., the 3D spin network states are the same as in 4D — they are $SU(2)$ spin networks. The difference is that in 3D they are made of trivalent graphs and in 4D with graphs with higher valence. Our discussion in the 3D model suggests that the topological observables can have similar role in 4D. The evolution of these 3D observables is expected to give the true dynamics in the full 4D theory. This can give an alternative route to explicit computations of the full spin foam amplitudes, which are a subject of recent interest [28,29]. It is also well known that the $\{6j\}_q$ symbols for $SU(2)_q$ give the exponential of the Einstein–Hilbert action in the limit of large spin quantum numbers, indicating a good semi-classical limit. In our case it will be interesting to investigate the limit with large cycles through the spin foam as well as the semi classical limit of the symbols from $SU(3)_q$ and $SU(N)_q$ in general.

We also presented a Lie algebra polytope interpretation of the transition amplitudes and observables, a "gravitahedra" [30] for spin foam quantum gravity. The representation theory polytopes emerge from the spin foam. This work opens up new questions for subsequent research such as questions on (1) phase transition and confinement within the anyonic code, (2) direct connection with particle physics observables and the notion of extended particle observables, (3) the complete formulation with larger Lie algebra amplitudes. The fifth root of unity also has limits on the large dimensional algebras which can be addressed — it stops at $SU(5) = A_4$ in the A_n series, for example. It will be interesting to investigate the tenth root of unity to incorporate larger Lie algebras as it also has a Fibonacci fusion Hilbert space structure.

The transition amplitudes, partition functions and observables discussed in this paper are all finite, which is supported by the tetrahedron quantization postulate to impose the fifth root of unity quantization. This quantization allows us to explicitly compute the amplitudes with some examples as well as to interpretate the pre-spacetime framework as a topological quantum computer. The universality of the simplest non-abelian (Fibonacci) anyon for quantum computation and its usefulness for explicitly computations of quantum gravity amplitudes motivates it as a start point postulate.

Declaration of competing interest

The authors declare that they have no known competing financial interests or personal relationships that could have appeared to influence the work reported in this paper.

[3] Note that we are using the same notation used for $SU(3)$ in previous sections, but the convex polytope possessing the symmetry of the Coxeter–Weyl group, as the orbit of its highest weight vector, by acting with $W(G_2)$, is a different polytope, a hexagon made of the two triangles of $SU(3)$, (10) and (01), and a point in the center, the (00) representation.

Appendix A. Review of spin foam models and its q-deformation regularization

Following [1], mainly chapters 5 and 6, we consider a discretization of spacetime in terms of a triangulation ($\triangle$) and its dual 2-complex ($\triangle^*$). A three-dimensional triangulation is given by tetrahedrons, triangles, segments and points. For a four-dimensional triangulation, we include the 4-simplex. The dual 2-complex in three-dimensional (3D) bulk is made by associating a tetrahedron with a vertex, a triangle with an edge, and a segment with a face. On the boundary, the dual of triangles are nodes and segments are links. In four dimensions (4D), the dual of a 4-simplex is a vertex, the dual of a tetrahedron is an edge and the dual of a triangle is a face. The boundary graph and terminology are equal to 3D. The gauge group of symmetry is $SU(2)$ in 3D, the covering group of the rotation group $SO(3)$, and $SL(2,C)$ or $SU(2)\times SU(2)$ in 4d, the respective covering groups of the Lorentz group and the 4D rotation group $SO(4)$. The variables are $SU(2)$ group elements U_e associated to edges e in the bulk of $\triangle^*$ or U_l associated to links l on the boundary, and algebra elements $L_f = L^i_f J_i$ associated to faces f of $\triangle^*$ or $L_l = L^i_l J_i$ associated to links on the boundary. J_i are the $SU(2)$ generators, $J_i = \frac{i}{2}\sigma_i$, where σ_i are the usual Pauli matrices. The quantization involves operators U_l and L_l on the boundary realizing a commutation relation on a Hilbert space,

$$\left[U_l, L^i_{l'}\right] = i\beta\delta_{ll'}U_l J^i \tag{A.1}$$

and

$$\left[L^i_l, L^j_{l'}\right] = i\beta\delta_{ll'}\epsilon^{ij}_k L^k_l, \tag{A.2}$$

where β is a constant related to the gravitational constant, $\delta_{ll'}$ is the Kronecker-delta and ϵ^{ij}_k is the totally antisymmetric Levi-Civita symbol. States are wavefunctions $\Psi(U_l)$ or $\Psi(L_l)$ of L group/algebra elements on L links of the boundary graph modulo the $SU(2)$ gauge symmetry implemented on the nodes. The Hilbert space is the space of square integrable functions of these coordinates:

$$\mathcal{H}_\Gamma = L_2\left[SU(2)^L/SU(2)^N\right]_\Gamma \tag{A.3}$$

where Γ is the boundary graph. The gauge invariant states must satisfy $\Psi(U_l) = \Psi\left(\lambda_{s_l}U_l\lambda^{-1}_{t_l}\right)$ for every node n of the boundary graph. One major realization of loop quantum gravity is that the kinematics are the same in 3D and 4D — the Hilbert space and commutation relations are in both cases the ones for the $SU(2)$ group. The distinction from 3D to 4D arises only in the dynamics, with the 4D gauge symmetry $SL(2,C)$ or $SU(2)\times SU(2)$ implemented on the bulk of the spin foam.

The dynamics are implemented in the form of a state sum model with quantum transition amplitudes or partition functions. Let us consider first the transition amplitude. It is a function of the states defined on $\Gamma = (\partial\triangle)^*$, the boundary graph. This can be defined in the group representation $W_\triangle(U_l)$ or in the so called spin representation $W_\triangle(j_f)$, where the $\triangle$ indicates that the amplitude is computed in a discretization $\triangle$ of the bulk that matches the boundary graph. In $W_\triangle(j_f)$, a basis on the gauge invariant Hilbert space is given by the normalized eigenvectors of the operator L_l, indicated by $|j_f\rangle$. An element of this basis is determined by assigning a spin j_l of a representation of $SU(2)$ to each link l of the graph. A graph with a spin assigned to each link is called a spin network. So the spin network states $|j_f\rangle$ form a basis of the gauge invariant Hilbert space of quantum gravity, i.e. they span the quantum states of the geometry. The quantum transition amplitude is given by

$$W_\triangle(j_l) = \mathcal{N}_\triangle \sum_{j_f}\prod_f A_{j_f}\prod_v A_v(j_f), \tag{A.4}$$

where $\mathcal{N}_\triangle$ is a normalization constant that can depend on the discretization, and there is an amplitude A_{j_f} for each face of $\triangle^*$ and an amplitude $A_v(j_f)$ for each vertex, both in 3D and 4D. Equivalently, in 3D, the amplitude A_{j_f} can be defined on the segments of $\triangle$ and $A_v(j_f)$ on the tetrahedrons[4]. Similarly, in 4D the amplitude A_{j_f} can be defined on the triangles of $\triangle$ and $A_v(j_f)$ on the 4-simplexes[5]. The partition function ($Z_\triangle$) in the situation with the triangulation without boundaries is the same as Eq. (A.4) but summing also over the boundary representations.

From now on we will consider the 3-dimensional spin foam model, but it was necessary to point out in the preceding review that the step from 3D to 4D is not a big one. In the spin network basis we have that the amplitudes A_{j_f} are given by the dimension of the representation, d_j, and the vertex amplitude $A_v(j_f)$, which implements the $SU(2)$ symmetry, is a function that takes the 6 spin quantum numbers of the representations on the 6 edges of the tetrahedron around a vertex and returns a complex number. The vertex amplitude in this case is given mainly by the Wigner 6j-symbol $\{6j\} = \begin{Bmatrix} j_1 & j_2 & j_3 \\ j_4 & j_5 & j_6 \end{Bmatrix}$,[6] and the transition amplitude is

$$W_\triangle(j_l) = \mathcal{N}_\triangle \sum_{j_f}\prod_f (-1)^{j_f} d(j_f)\prod_v (-1)^{j_v}\{6j\}, \tag{A.5}$$

where $j_v = \sum_{a=1}^6 j_a$.

Note that even with the definition of this object on a truncation of the triangulation, still there are non-physical divergences. We see this by first writing explicitly Eq. (A.5) for a triangulation made of 1 tetrahedron. The dual is made of a vertex inside the tetrahedron connected to a node on each of the 4 triangular faces. The dual has 6 boundary faces that we label with 6 $SU(2)$ representations (or equivalently there is a dual tetrahedron and the representations are living on its edges) and the transition amplitude is immediately

$$W_{\triangle_1}(j_l) = (-1)^{j_v}\begin{Bmatrix} j_1 & j_2 & j_3 \\ j_4 & j_5 & j_6 \end{Bmatrix} \tag{A.6}$$

and is well defined, although for the partition function one should sum over the infinite number of $SU(2)$, j_f, representations. The problem for transition amplitudes already occurs for the triangulation with only four tetrahedrons, made by inserting a point inside the initial large one and connecting it with the 4 tetrahedron points. The dual is made of four vertices inside the 4 tetrahedrons connected with each other and the boundary faces. Now there are the 6 boundary faces with representations labeled $j_1 \ldots j_6$, plus 4 internal faces, $j_7 \ldots j_{10}$, of the dual, (see Fig. A.2). What happens is that even with the 6 boundary spin representations fixed, the classical $SU(2)$ fusion rules do not give a constraint on the spin representations on these internal faces, and the amplitude can diverge

$$W_{\triangle_4}(j_1,\ldots,j_6) = \sum_{j_f}\prod_{f=1}^{10}(-1)^{j_f} d(j_f)\prod_{v=1}^{4}(-1)^{j_v}\{6j\}, \tag{A.7}$$

where each $\{6j\}$ now has 3 boundary spin representations and 3 internal ones. These internal spins are not fixed by triangular inequalities. All the four internal spins form an internal tetrahedron where the spins can flow without restriction — the tetrahedron with the vertices 1, 2, 3 and 4 in Fig. A.2. From results of LQG, the spin quantum numbers correspond to eigenvalues of geometrical operators such as lengths and areas, and so there is a divergence when the scale of the geometry becomes large, a kind of infrared divergence. This is possible because in Riemannian geometry the space can be strongly curved. The 4 internal faces form what is called a bubble in LQG, and the divergence for a large spin sitting on an internal triangular face is called a spike.

[4] The input for $A_v(j_f)$ are the representations on each one of the 6 faces adjacent to the vertex or the representations on the 6 segments that form the tetrahedron. We can note that $A_v(j_f)$ comes from a path integral quantization and gives the weighted value of the field at one point of the discretization.

[5] The 4-simplex has 10 edges and 10 triangles, so the input for $A_v(j_f)$ are 10 representations. The boundary graph of the amplitude is a pentagram.

[6] See [1] for explicit definitions.

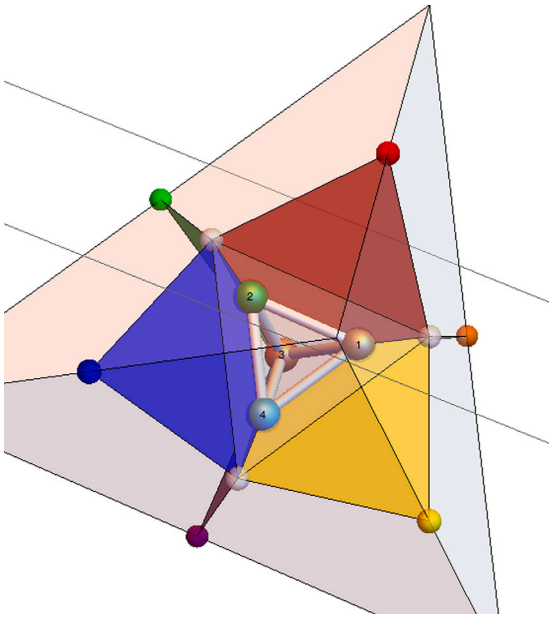

Fig. A.2. The dual 2-complex for the triangulation level 1 with four tetrahedrons, highlighting the external faces.

The transition amplitudes can be made well defined and explicitly independent of the triangulation by a deformation of the $SU(2)$ symmetry, using quantum $SU(2)_q$ with a deformation parameter q defined as a complex root of unity $q = e^{\frac{2\pi i}{r}}$, with r an integer.[7]. The transition amplitudes is given by

$$W_q(j_l) = \mathcal{N}_q \sum_{j_f} \prod_f (-1)^{j_f} d_q(j_f) \prod_v (-1)^{j_v} \{6j\}_q, \tag{A.8}$$

where we have now, as the quantum-deformed analogues of the objects that appear in the transition amplitude, the quantum dimension $d_q(j_f)$ and the quantum Wigner 6j-symbol $\{6j\}_q = \left\{ \begin{array}{ccc} j_1 & j_2 & j_3 \\ j_4 & j_5 & j_6 \end{array} \right\}_q$. From the representation theory of quantum groups [31] we know that the spin quantum numbers of $SU(2)_q$ are constrained to $j \leq \frac{r-2}{2}$, working as a cut off for the flow of spin on the bubbles. The usual triangular inequalities are modified and supplemented by the conditions $2j_1, 2j_2, 2j_3 \leq j_1 + j_2 + j_3 \leq r - 2$, which are the triangular inequalities of a triangle on a sphere with a radius determined by r. The geometry of q-deformed spin networks is therefore consistent with the geometry of constant curvature space, with the curvature determined by the specific root of unity.

Our particular synthesis of this result is that a general large spin transition amplitude should be built from "gluing" quantum building blocks $W_{\triangle_1}$ given by $\{6j\}_q$ with a specific q that fixes $W_{\triangle_1}$ to low spin representations, and we discussed and justified the choice of $q = e^{\frac{2\pi}{5} i}$ in the main text.

Appendix B. Gauge grand unification physics review

Let us provide a short review of the Lie algebra unification physics program closely following the Refs. [4–6]. The well known representation theory of $SU(2)$ can be extended to higher dimensional Lie groups and algebras. The structure of a simple Lie algebra is described by its root and weight systems. The classification of simple Lie algebras is an extensive subject on which we recommend the Refs. [4,7,8]. Here we collect and review just the elements necessary for our discussion. For example we have that the root system A_n describes $SU(n+1)$, while D_n, with $n \geq 3$, describes the Lie algebra of $SO(2n)$. The exceptional Lie algebras G_2, F_4, E_6, E_7 and E_8 have their root systems with the same respective names. For our discussion we will focus on A_n, in particular A_2, and E_8, whose importance for coupling the charge space with spin foam was pointed out in [32], and which contains the other exceptional Lie algebras as well the A_n for lower n.

[7] See chapter 6 of [1].

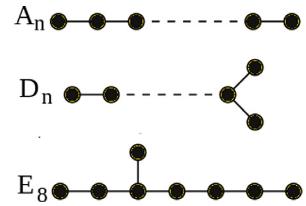

Fig. B.3. Coxeter—Dynkin diagrams of A_n, D_n and E_8.

Let us consider a Euclidean space V of dimension n. One can introduce an orthonormal basis, l_i $(i = 1, 2, \ldots, n)$, in V so that the Euclidean scalar product (u, v) of $u = \sum_i \lambda_i l_i$ and $v = \sum_i \mu_i l_i$ is $(u, v) = \sum_i \lambda_i \mu_i$. The Coxeter—Dynkin diagrams of A_n, D_n and E_8 are shown in Fig. B.3. The nodes on the Coxeter—Dynkin diagram represent the simple roots α_i, $(i = 1, 2, \ldots, n)$, of the associated Lie algebra of rank n[8] and two dots linked by an edge correspond to two roots whose scalar product is -1. The other pairs of nodes, which are not connected, correspond to vectors that are orthogonal. The Cartan matrix elements are

$$C_{ij} = \frac{2(\alpha_i, \alpha_j)}{(\alpha_j, \alpha_j)}. \tag{B.1}$$

Complementary to the simple roots, there are the fundamental weight vectors ω_i, which are defined by the relation with the simple roots $(\omega_i, \alpha_j) = \delta_{ij}$ and are related to each other by $(\omega_i, \omega_j) = (C^{-1})_{ij}$. The root lattice Λ is the set of vectors $p = \sum_i^n b_i \alpha_i$, $b_i \in \mathbb{Z}$. Similarly the weight lattice Λ^* is the set of vectors $q = \sum_i^n p_i \omega_i$, $p_i \in \mathbb{Z}$. The reflection generator with respect to the hyperplane orthogonal to the simple root α_i is r_i, $(i = 1, \ldots, n)$, which operates on an arbitrary vector λ as

$$r_i \lambda = \lambda - \frac{2(\lambda, \alpha_i)}{(\alpha_i, \alpha_i)} \alpha_i. \tag{B.2}$$

It transforms a fundamental weight vector as $r_i \omega_j = \omega_j - \alpha_i \delta_{ij}$. These generators form the Coxeter reflection group (Weyl group) acting on the root system G defined by the presentation $W(G) = \langle r_1, \ldots, r_n | (r_i r_j)^{m_{ij}} = 1 \rangle$. When they act on one of the simple roots of a simple Lie algebra they generate the root system $W(G)\alpha_i$.

The concept of polytopes is important to our discussion. The root polytope is a convex polytope whose vertices are vectors of the root system. The highest weight vector for an irreducible representation of the Lie algebra is defined as the weight vector $\omega_{rep} = (p_1, \ldots, p_n)$, where p_i are positive integers called Dynkin labels. The highest weight of any irreducible representation decomposes on fundamental weights, and its components are its Dynkin labels

$$\omega_{rep} = \sum_i p_i \omega_i. \tag{B.3}$$

The highest weight vector has an associated polytope, which is the convex polytope possessing the symmetry of the Coxeter–Weyl group as the orbit of this highest weight vector $W(G)(p_1, \ldots, p_n) = (p_1, \ldots, p_n)_g$. With this notation the root polytope of $W(A_n)$ is given, in a simplified form, as $(10...01)_{A_n}$. For A_2, for example, (11) describes the root polytope, the hexagon with 2 points in the middle in Fig. B.4, and each point

[8] An N dimensional Lie algebra is a vector space which contains an n dimensional subspace, the so called **Cartan subalgebra**, spanned by a maximal set of n inter-commuting generators, H_a, $[H_a, H_b] = 0 \quad \forall \quad 1 \leq a, b \leq n$.

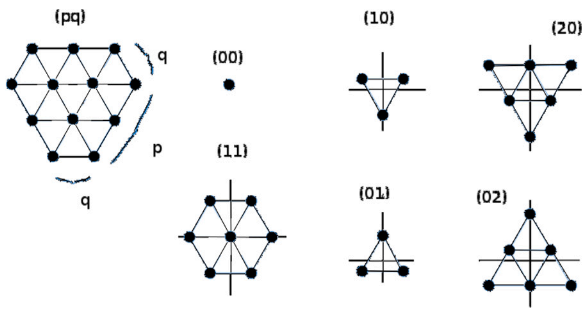

Fig. B.4. A_2 "polytopes".

corresponds to one of the 8 states of the adjoint representation, so (11) can refer also to the whole adjoint representation. The fundamental simplex of the lattice A_n is a convex polytope with $n+1$ vertices given by $\omega_1, \ldots, \omega_n$ and the origin (0). The Voronoi polytope $V(0)$ centered at the origin of the lattice Λ is the set of points $V(0) = \left\{ x \in \mathbb{R}^n, \forall p, (x,p) \leq \frac{1}{2}(p,p) \right\}$. Let $v \in \mathbb{R}^n$ be a vertex of an arbitrary Voronoi polytope $V(p)$. The convex hull of the lattice points closest to v is called the Delone polytope containing v. Vertices of the Voronoi cell $V(0)$ of the root lattices of the A_n series consist of the vertices of the Delone cells centered at the origin.

Let us show the analogue of these polytopes in lower dimension for $A_1 = SU(2)$. First we will write the eigenvalues in integer form, $p = 2j$ and then:

- $p = 1$ is the highest weight of the fundamental representation with one reflection that sends it to the state $p = -1$. The edge from the $p = -1$ to $p = 1$ is the Voronoi polytope, written (1) in the notation above.
- With $p = 2$, operating with the $W(A1)$ one gets the other 2 states of the adjoint representation, $p = 0$ and $p = -2$. The edge from $p = -2$ to $p = 2$ forms the root polytope which is the dual of the Voronoi polytope, and is represented as (2), which also indicates the adjoint representation.
- Note that the building block is the Delone polytope which is an edge of length 1.

For A_2 we present the representations of interest in Fig. B.4, and note that the Voronoi cell is the hexagon made of the 2 triangles (10) and (01), while the Delone cell's building blocks are the triangles whose centers are the vertices of the Voronoi cell. Each one is equivalent to one of the triangles (10) and (01) - and six of them make the hexagon root polytope.

It is not necessary to introduce the polytopes of the exceptional Lie algebras because we will work with G_2 and E_8 only as a container for the interaction between its A_2 subalgebras, which will be our main objects.

To present a general representation of the roots and the weights of A_n we add one vector to our orthonormal set of vectors, l_i ($i = 1, 2, \ldots, n+1$), $(l_i, l_j) = \delta_{ij}$. We define the simple roots as linear combinations of orthonormal vectors $\alpha_i = l_i - l_{i+1}$, ($i = 1, 2, \ldots, n$). The group generators r_i permute the set of orthonormal vectors as $r_i : l_i \leftrightarrow l_{i+1}$. When we define the vectors in terms of their components in the $n+1$ dimensional Euclidean space the simple roots and the fundamental weights read

$$\begin{aligned}
\alpha_1 \;&=\; (1,-1,0,\ldots,0); \ldots; \alpha_n = (0,0,\ldots,1,-1);\\
\omega_1 &= \frac{1}{n+1}\,(n,-1,\ldots,-1); \omega_2 = \frac{1}{n+1}(n-1,n-1,-2,\ldots,-2);\\
\ldots;\quad \omega_n &= \frac{1}{n+1}(1,1,\ldots,1,-n).
\end{aligned} \tag{B.4}$$

For $SU(3)$ we have the simple roots and weights

$$\begin{aligned}
\alpha_1 &= (1,-1,0),\\
\alpha_2 &= (0,1,-1),\\
\omega_1 &= (2/3,-1/3,-1/3),\\
\omega_2 &= (1/3,1/3,-2/3).
\end{aligned} \tag{B.5}$$

They can be used to compute the scalar products on the amplitudes discussed below.

The derivation of the Lie algebra from its root system is standard. Let us consider the generalization of Eq. (2) for $SU(2)$ to $SU(3)$. To each of the 2 simple roots α_i we associate three generators h_i, L_i^+ and L_i^-. These generate the $SU(3)$ algebra subject to the relations

$$\begin{aligned}
\left[h_i, h_j\right] &= 0\\
\left[h_i, L_j^{\pm}\right] &= \pm C_{ij} L_j^{\pm}\\
\left[L_i^{+}, L_j^{-}\right] &= \delta_{ij} h_j,\\
\left[L_i^{\pm}, \left[L_i^{\pm}, L_j^{\pm}\right]\right] &= 0, \qquad i \neq j
\end{aligned} \tag{B.6}$$

where, from Eq. (B.1), $C_{ij} = -1 + 3\delta_{ij}$. The Cartan–Weyl basis, or in this situation the Chevalley basis, allows us to write the large dimensional Lie algebra in terms of the relationship between its building block $SU(2)$ subalgebras.

References

[1] C. Rovelli, F. Vidotto, Covariant Loop Quantum Gravity, first ed., Cambridge University Press, 2014.

[2] M.B. Green, J.H. Schwarz, E. Witten, Superstring Theory, Vol. I and II, Cambridge University Press, 1988.

[3] K. Becker, M. Becker, J.H. Schwarz, String Theory and M-Theory - A Modern Introduction, Cambridge University Press, 2007.

[4] H. Georgi, Lie Algebras in Particle Physics. from Isospin Fo Unified Theories, second ed., Westview Press, 1999.

[5] M. Koca, N.Ozdes. Koca, A. Al-Siyabi, R. Koca, Explicit construction of the voronoi and delaunay cells of W(An) and W(Dn) lattices and their facets, Acta. Cryst. A Found Adv. 74 (Pt 5) (2018) 499–511.

[6] M. Koca, N.Ozdes. Koca, A. Al-Siyabi, Su(5) grand unified theory, its polytopes and 5-fold symmetric aperiodic tiling, Int. J. Geom. Methods Mod. Phys. (IJGMMP) 15 (4) (2018).

[7] A. Zee, Group Theory in a Nutshell for Physicists, Princeton University Press, 2016.

[8] R. Gilmore, Lie Groups, Lie Algebras, and Some of their Applications, Dover publications, INC., 2005.

[9] A.G. Lisi, An exceptionally simple theory of everything, 2007, arXiv:0711.0770 [hep-th].

[10] C. Castro, A clifford algebra-based grand unification program of gravity and the standard model: a review study, Can. J. Phys. 92 (12) (2014) 1501–1527, http://dx.doi.org/10.1139/cjp-2013-0686.

[11] B. Baytas, E. Bianchi, N. Yokomizo, Gluing polyhedra with entanglement in loop quantum gravity, Phys. Rev. D 98 (2018) 026001, arXiv:1805.05856 [gr-qc].

[12] M.V. Raamsdonk, Building up spacetime with quantum entanglement II: It from BC-bit, 2018, arXiv:1809.01197 [hep-th].

[13] Z. Wang, Topological Quantum Computation, Number 112, American Mathematical Soc., 2010.

[14] J.K. Pachos, Introduction To Topological Quantum Computation, Cambridge University Press, 2012.

[15] A. Barbieri, Quantum tetrahedra and simplicial spin networks, Nuclear Phys. B 518 (1998) 714–728, arXiv:gr-qc/9707010.

[16] M. Amaral, K. Irwin, On the poincaré group at the 5th root of unity, 2019, http://dx.doi.org/10.20944/preprints201903.0137.v1, Preprints 2019, 2019030137.

[17] V.G. Turaev, O.Y. Viro, State sum invariants of 3-manifolds and quantum 6j-symbols, Topology 31 (4) (1992) 865–902.

[18] M.A. Nielsen, I.L. Chuang, Quantum Computation and Quantum Information, Cambridge University Press, Cambridge, UK., 2000.

[19] M. Freedman, M. Larsen, Z. Wang, A modular functor which is universal for quantum computation, Comm. Math. Phys. 227 (605) (2002).

[20] E. Bianchi, M. Han, C. Rovelli, W. Wieland, E. Magliaro, C. Perini, Spin-foam fermions, Classical Quantum Gravity 30 (2013) 235023, arXiv:1012.4719 [gr-qc].

[21] Z. You-jin, A remark on the representation theory of the algebra uq(sl(n)) when q is a root of unity, J. Phys. A Math. Gen. V. 25 (4) (1992) 851.

[22] E. Ardonne, J.K. Slingerland, Clebsch–Gordan and 6j-coefficients for rank two quantum groups, J. Phys. A 43 (2010) 395205, arXiv:1004.5456 [math.QA].

[23] A.N. Kirillov, N.Y. Reshetikhin, Representations of the algebra uq(sl(2)), q-orthogonal polynomials and invariants of links, in: V.G. Kac (Ed.), Infinite Dimensional Lie Algebras and Groups, Proceedings of the Conference Held At CIRM, Luminy, Marseille, World Scientific, Singapore, 1988, p. 285.

[24] Satoshi Nawata, Ramadevi Pichai, Zodinmawia, Multiplicity-free quantum 6j-symbols for $U_q(sl_N)$, Lett. Math. Phys. 103 (12) (2013) 1389.

[25] Markus Kuhn, Hans Walliser, Program for calculating SU(4) Clebsch–Gordan coefficients, Comput. Phys. Comm. 179 (10) (2008) 733.

[26] J.M. Garcia-Islas, Observables in 3-dimensional quantum gravity and topological invariants, Classical Quantum Gravity 21 (2004) 3933–3952, arXiv:gr-qc/0401093.

[27] P. Truini, A. Marrani, M. Rios, Magic star and exceptional periodicity: an approach to quantum gravity, J. Phys. Conf. Ser. 1194 (1) (2019) 012106, arXiv:1811.11202 [hep-th] (2019).

[28] P. Dona, G. Sarno, Numerical methods for EPRL spin foam transition amplitudes and Lorentzian recoupling theory, Gen. Relativ. Gravit. 50 (2018) 127, arXiv:1807.03066 [gr-qc].

[29] G. Sarno, S. Speziale, G.V. Stagno, Gen. Relativ. Gravit. 50 (43) (2018) http://dx.doi.org/10.1007/s10714-018-2360-x.

[30] P. Truini, Vertex operators for an expanding universe, AIP Conference Proceedings 2150 (040005) (2019) arXiv:1901.07916 [physics.gen-ph].

[31] L.C. Biedenharn, M.A. Lohe, Quantum Group Symmetry and Q-Tensor Algebras, World Scientific, 1995.

[32] R. Aschheim, SpinFoam with topologically encoded tetrad on trivalent spin networks, in: International Conference on Non-perturbative / background independent quantum gravity (Loops 11): Madrid, Spain, 2011, Madrid arXiv:1212.5473 [cs.IT] (2011).